

CALCIUM GRADIENTS AND BUFFERS IN BOVINE CHROMAFFIN CELLS

BY ERWIN NEHER AND GEORGE J. AUGUSTINE*

*From the Max Planck Institute for Biophysical Chemistry, Am Fassberg, D-3400 Göttingen, Germany and the *Department of Neurobiology, Duke University Medical Center, Post Office Box 3209, Durham, NC 27710, USA*

(Received 29 April 1991)

SUMMARY

1. Digital imaging and photometry were used in conjunction with the fluorescent Ca^{2+} indicator, Fura-2, to examine intracellular Ca^{2+} signals produced by depolarization of single adrenal chromaffin cells.

2. Depolarization with a patch pipette produced radial gradients of Ca^{2+} within the cell, with Ca^{2+} concentration highest in the vicinity of the plasma membrane. These gradients dissipated within a few hundred milliseconds when the voltage-gated Ca^{2+} channels were closed.

3. Dialysis of Fura-2 into the chromaffin cell caused concentration-dependent changes in the depolarization-induced Ca^{2+} signal, decreasing its magnitude and slowing its recovery time course. These changes were used to estimate the properties of the endogenous cytoplasmic Ca^{2+} buffer with which Fura-2 competes for Ca^{2+} .

4. The spatially averaged Fura-2 signal was well described by a model assuming fast competition between Fura-2 and an endogenous buffer on a millisecond time scale. Retrieval of calcium by pumps and slow buffers occurs on a seconds-long time scale. No temporal changes indicative of buffers with intermediate kinetics could be detected.

5. Two independent estimates of the capacity of the fast endogenous Ca^{2+} buffer suggest that 98–99% of the Ca^{2+} entering the cell normally is taken up by this buffer. This buffer appears to be immobile, because it does not wash out of the cell during dialysis. It has a low affinity for Ca^{2+} ions, because it does not saturate with $1\ \mu\text{M}$ Ca^{2+} inside the cell.

6. The low capacity, affinity and mobility of the endogenous Ca^{2+} buffer makes it possible for relatively small amounts of exogenous Ca^{2+} buffers, such as Fura-2, to exert a significant influence on the characteristics of the Ca^{2+} concentration signal as measured by fluorescence ratios. On the other hand, even at moderate Fura-2 concentrations (0.4 mM) Fura-2 will dominate over the endogenous buffers. Under these conditions ratiometric Ca^{2+} concentration signals are largely attenuated, but absolute fluorescence changes (at 390 nm) accurately reflect calcium fluxes.

INTRODUCTION

Transient rises in intracellular Ca^{2+} concentration, $[\text{Ca}^{2+}]_i$, are signals for exocytosis in many secretory cells (Douglas, 1968; Katz, 1969; Parnas, Dudel & Parnas, 1982; Augustine, Charlton & Smith, 1987; Penner & Neher, 1988). The magnitude and spatiotemporal distribution of these $[\text{Ca}^{2+}]_i$ signals are a consequence of the interplay between cellular Ca^{2+} sources and Ca^{2+} removal mechanisms (Zucker, 1989; Sala & Hernandez-Cruz, 1990). In adrenal chromaffin cells, depolarization-induced $[\text{Ca}^{2+}]_i$ signals are due to Ca^{2+} entry through voltage-gated Ca^{2+} channels (Fenwick, Marty & Neher, 1982; Knight & Kesteven, 1983; O'Sullivan, Cheek, Moreton, Berridge & Burgoyne, 1989) and perhaps additional release of Ca^{2+} from internal stores (O'Sullivan *et al.* 1989). Cells remove Ca^{2+} via a variety of mechanisms, including transmembrane Na^+ - Ca^{2+} exchange (Pocock, 1983) and Ca^{2+} sequestration into organelles via ATP-driven pumps (Burgoyne, Cheek, Morgan, O'Sullivan, Moreton, Berridge, Mata, Colyer, Lee & East, 1989). By analogy with other cells (Brinley, 1978), it is likely that chromaffin cells also possess cytoplasmic Ca^{2+} buffers but these have not yet been characterized.

The previous paper quantified the Ca^{2+} requirements for secretion in chromaffin cells and showed that depolarization produces substantial changes in $[\text{Ca}^{2+}]_i$ at secretory sites (Augustine & Neher, 1992). The discrepancy between the magnitudes of the $[\text{Ca}^{2+}]_i$ levels deduced to be present at the secretory sites and actual measurements of spatially averaged $[\text{Ca}^{2+}]_i$ signals suggested that spatial gradients occur during stimulation. In this paper we use the fluorescence Ca^{2+} indicator, Fura-2 (Grynkiewicz, Poenie & Tsien, 1985), and digital microscopy to examine more directly the spatiotemporal properties of the $[\text{Ca}^{2+}]_i$ signal evoked by depolarization. We demonstrate that $[\text{Ca}^{2+}]_i$ gradients are present during stimulation. We also examine the properties of the endogenous Ca^{2+} buffer that shapes the $[\text{Ca}^{2+}]_i$ signal and find that this buffer normally binds most of the Ca^{2+} entering the cell. However, because this buffer is immobile and does not saturate at $[\text{Ca}^{2+}]_i$ levels as high as $1 \mu\text{M}$, the addition of exogenous buffers, such as Fura-2, can alter the form of the $[\text{Ca}^{2+}]_i$ signal measured during depolarization. A preliminary report of some of this work has appeared (Augustine & Neher, 1990).

METHODS

The methods used for patch clamp recording from single chromaffin cells are described in the previous paper (Augustine & Neher, 1991). The standard internal dialysis solution contained (in mM): 145 caesium glutamate, 8 NaCl, 1 MgCl_2 , 2 Mg-ATP, 0.3 GTP, 10 Na-HEPES (pH 7.2) and a variable amount of K_2 -EGTA and/or K-Fura-2 (Molecular Probes, Eugene, OR, USA). In imaging experiments, 0.5 mM-EGTA was used in conjunction with 0.1–0.5 mM-Fura-2. Other experiments used no added EGTA and 0.05–0.4 mM-Fura-2. The external solution contained (in mM): 120 NaCl, 2–5 CaCl_2 , 20 tetraethylammonium-chloride, 2 MgCl_2 , 50 glucose, 10 Na-HEPES (pH 7.2), and 1 μM -tetrodotoxin (TTX).

Imaging of $[\text{Ca}^{2+}]_i$ signals

Digital imaging methods were used, in combination with Fura-2, to examine spatial gradients in $[\text{Ca}^{2+}]_i$ in single chromaffin cells during depolarization. Conventional ratiometric measurements of $[\text{Ca}^{2+}]_i$ with Fura-2 require alternation of the excitation light source between two wavelengths (Tsien & Poenie, 1986). However, the temporal resolution of this method is limited, because of the

time required for switching the wavelength of the excitation light and for acquiring images at each of the two wavelengths. In order to minimize the time resolution of our measurements, we used a single-excitation wavelength ratio method (Smith, Osse & Augustine, 1988). In this method, the Fura-2 is excited at a single, Ca^{2+} -sensitive wavelength, in our case 390 nm (10 nm bandpass), and

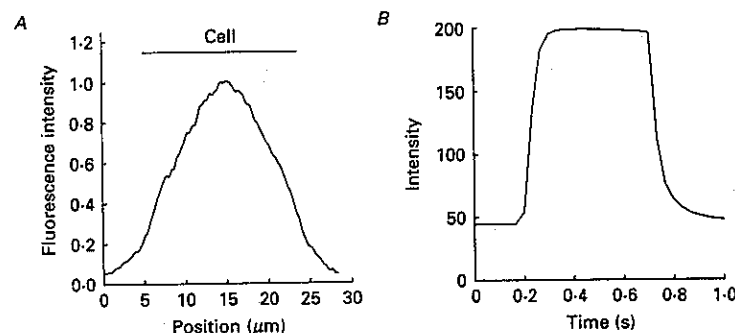


Fig. 1. Spatial and temporal resolution of the video microscope system. *A*, the spatial resolution was determined by examining the fluorescence intensity profile of a chromaffin cell loaded with Fura-2 via a patch pipette. Fluorescence was measured along a line perpendicular to the long axis of the patch pipette, including the region occupied by the cell (indicated by bar). Fluorescence was not uniform within the cell and extended several micrometres beyond the edges of the cell. *B*, the temporal resolution of the system was determined by the response to a brief flash of green light from a light-emitting diode.

the changes in Fura-2 fluorescence emission (at 500–530 nm), $\Delta F(t)$, are measured following a stimulus that elevates $[\text{Ca}^{2+}]_i$. To correct for non-uniformities in path length and dye concentration, $\Delta F(t)$ is divided by the pre-stimulus fluorescence, $F(0)$. Thus, the ratio is:

$$\Delta F(t)/F(0) = (F(t) - F(0))/F(0), \quad (1)$$

where $F(t)$ is the fluorescence at any time later than the time at which $F(0)$ was measured. Such a ratio is a unique function of the stimulus-induced change in $[\text{Ca}^{2+}]_i$ (see eqn (3), below) as long as the path length and Fura-2 concentration do not change during the measurement. In the experiments reported here, there were no obvious stimulus-dependent changes in path length (measured when exciting at 360 nm, the isostilbic (Ca^{2+} -independent) wavelength of Fura-2). Dye concentration was kept constant both by waiting until dialysis of Fura-2 into the cells had reached a maximum (typically 60–120 s after establishing continuity between the pipette and cytoplasm) and by avoiding bleaching of the dye through the use of a quartz neutral density filter (10–50% transmission) and a Uniblitz (Rochester, NY, USA) electronic shutter in the fluorescence excitation optical path to minimize illumination of the Fura-2.

The apparatus used to obtain digital images of $[\text{Ca}^{2+}]_i$ changes was similar to that described in Smith *et al.* (1988) and Kasai & Augustine (1990). In brief, an inverted microscope (Zeiss IM-35) fitted with a 100 \times oil immersion objective (Zeiss Plan 100, numerical aperture = 1.25) was used to excite the intracellular Fura-2 and collect the resultant fluorescence signals. The size of the illumination beam was kept to a minimum (*ca* 30 μm diameter) with a diaphragm, in order to minimize the depth of field of the fluorescence measurements (Hiraoka, Sedat & Agard, 1990). Fluorescence signals measured with Fura-2 in the cells, as well as background signals measured before Fura-2 was dialysed into the cells, were acquired with a SIT video camera (Cohu, model 5000) and the video images were stored on an analog, optical disc storage device (Panasonic TQ-2026F). These images were then digitized off-line, using a Matrox MVP-AT frame grabber in an AST Premium 286 computer, and manipulated with computer programs written in C language by Stephen J. Smith. Eight-bit pseudocolour look-up tables were used to encode the magnitude of the

$\Delta F(t)/F(0)$ signals within each element of the 480×512 pixel array (see Fig. 4). The resultant pseudocolor maps were then masked to exclude extracellular fluorescence signals. The boundaries of the mask were determined by an intensity threshold, with the value of this threshold adjusted until the non-masked area corresponded to the area occupied by the cell, as determined from bright field images.

The effective spatial and temporal resolutions of the entire optical system were assessed independently. Spatial resolution was estimated from the profile of fluorescence in a cell loaded with Fura-2. The fluorescence within the cell was not uniform (Fig. 1A), due to the spherical geometry of the cell and the tendency of Fura-2 signals to be brightest in the nuclear region of the cell (see Results). In addition, the fluorescence signal extended beyond the boundaries of the cells (determined from examination under bright-field illumination), due to blurring. The lateral resolution of the system, measured from the distance required for this extracellular fluorescence to decay to half of its maximum, was approximately $2-3 \mu\text{m}$ (Fig. 1A). The temporal resolution of the system was determined by putting a green light-emitting diode in the optical pathway and recording the response to light emitted by a current pulse 500 ms in duration. The time required for the recorded light signal to rise from 10–90% of its maximum was in the order of 100 ms (Fig. 1B), with similar values also measured during the decay of the light signal. Similar response times were observed when Fura-2-loaded cells were briefly illuminated by transiently opening the electronic shutter. The temporal response of the system presumably is limited by the SIT video camera (Inoue, 1986).

In single-wavelength measurements with Fura-2 at 390 nm, if the dye concentration, path length and intensity of excitation light are constant, then the fluorescence signal will lie between two extremes – F_{min} , the fluorescence of the dye when completely bound to Ca^{2+} , and F_{max} , the fluorescence when completely unbound to Ca^{2+} . The relationship between Ca^{2+} concentration, $[\text{Ca}^{2+}]_i$, and fluorescence intensity (F) is:

$$[\text{Ca}^{2+}]_i = K_D (F_{\text{max}} - F) / (F - F_{\text{min}}), \quad (2)$$

where K_D is the dissociation constant for Ca^{2+} binding to Fura-2. Combining eqns (1) and (2) yields the following expression for the fluorescence change ratio:

$$\frac{\Delta F(t)}{F(0)} = \frac{(K'_D + [\text{Ca}^{2+}]_{i,t}) / (K_D + [\text{Ca}^{2+}]_{i,t}) - 1}{(K'_D + [\text{Ca}^{2+}]_{i,0}) / (K_D + [\text{Ca}^{2+}]_{i,0}) - 1}, \quad (3)$$

where $[\text{Ca}^{2+}]_{i,0}$ is the initial (resting) value of $[\text{Ca}^{2+}]_i$, $[\text{Ca}^{2+}]_{i,t}$ is the value of $[\text{Ca}^{2+}]_i$ during a response, and

$$K'_D = K_D (F_{\text{max}} / F_{\text{min}}). \quad (4)$$

This relationship permits changes in fluorescence ratio to be converted into absolute $[\text{Ca}^{2+}]_i$ levels by solving for $[\text{Ca}^{2+}]_{i,t}$. This requires knowledge of $[\text{Ca}^{2+}]_{i,0}$, which was determined experimentally by alternately exciting the cell with 390 and 360 nm light and calculating the ratio of emission produced by the two wavelengths. This ratio was converted into $[\text{Ca}^{2+}]_{i,0}$ using the calibration procedure described in Neher (1989).

We directly tested the validity of this strategy by measuring the changes in fluorescence produced by depolarization of cells dialysed with $100 \mu\text{M}$ -Fura-2. These cells were alternately excited at either 390 or 360 nm, using the filter wheel described in Neher (1989), and 2-wavelength ratios were calculated from the resultant fluorescence signals. This was then used to calculate $[\text{Ca}^{2+}]_{i,t}$, as described by Neher (1989) and Augustine & Neher (1992). These signals were then compared to single-wavelength ratios of $\Delta F(t)/F(0)$, measured from the 390 nm signals produced during the same trials used to calculate $[\text{Ca}^{2+}]_{i,t}$ with the 2-wavelength method. The relationship between $[\text{Ca}^{2+}]_{i,t}$ and $\Delta F(t)/F(0)$ is shown for two different cells in Fig. 2. One cell had a $[\text{Ca}^{2+}]_{i,0}$ of 100 nM and the other had a resting $[\text{Ca}^{2+}]_{i,0}$ of 270 nM. The predictions of eqn (3) are also plotted for $[\text{Ca}^{2+}]_{i,0}$ of 100 or 270 nM (smooth lines). The close correspondence of the experimental values to the predictions of the equation verifies the calibration scheme for the single-wavelength ratios.

Measurement of the Ca^{2+} binding properties of cytoplasm

Fura-2 signals under whole-cell patch clamp conditions. In many neurone-like cells, $[\text{Ca}^{2+}]_i$ rapidly increases during depolarization (in the 10–100 ms time range) and then recovers over a much slower time scale (typically in the range of tens of seconds; Thayer & Miller, 1990; Hernandez-Cruz, Sala

& Adams, 1990). The peak change in $[\text{Ca}^{2+}]_i$ is orders of magnitude lower than would be expected if all the Ca^{2+} entering the cell was free and distributed evenly in the cell volume (McBurney & Neering, 1985). Thus, there must be fast Ca^{2+} buffers in addition to the slow uptake and removal systems which govern the recovery time course. Since the two processes are kinetically well

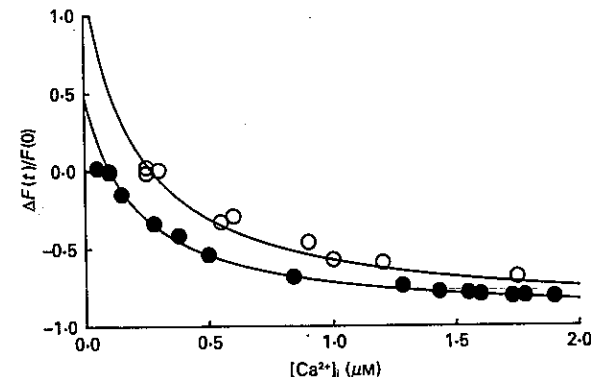


Fig. 2. Comparison of Fura-2 measurements made with single- and dual-wavelength ratio methods. Points represent $[\text{Ca}^{2+}]_i$ changes elicited by brief depolarizations; ● indicate measurements made from a cell with a resting $[\text{Ca}^{2+}]_i$ of 100 nM and ○ indicate measurements from a second cell with a resting $[\text{Ca}^{2+}]_i$ of 270 nM. Abscissa is $[\text{Ca}^{2+}]_i$ calculated from dual excitation-wavelength ratios and ordinate is fractional change in fluorescence at a single excitation wavelength, 390 nm. Continuous lines are plots of eqn (3) with $K_D = 150$ nM, the value obtained from chromaffin cell cytoplasm using eqn (16) (see below) and $K'_D = 8.97 \mu\text{M}$, which was empirically determined for the apparatus used to make these measurements.

separated (Thayer & Miller, 1990; see also Fig. 7), for the purpose of a kinetic model it is reasonable to distinguish fast Ca^{2+} buffers, which are essentially at equilibrium, and slow ones, in which all pumps, exchange carriers and slow binding sites are 'lumped' together, as has been done for other preparations (Melzer, Rios & Schneider, 1986).

In the case where a patch pipette is used to deliver Fura-2 to the interior of a cell, the fast buffering system competes with the Fura-2 (which has binding kinetics in the millisecond time range, Kao & Tsien, 1988) and the slow process competes with diffusion of Ca^{2+} and Ca^{2+} buffers (including Fura-2) into and out of the pipette. Such a situation is depicted in Fig. 3. It was treated by Mathias, Cohen & Oliva, 1990, in a more general form. Their eqn (A 7) describes the kinetics of Ca^{2+} changes (with conservation of total calcium):

$$d[\text{Ca}^{2+}]_i/dt + d[\text{BCa}]/dt + d[\text{SCa}]/dt = (j_{\text{in}} - j)/v, \quad (5)$$

where $[\text{BCa}]$ is the concentration of a mobile buffer (such as Fura-2) in its Ca-bound form, $[\text{SCa}]$ is the concentration of fixed (endogenous) Ca^{2+} buffer in the calcium-bound form, and v is the accessible volume of the cell. For the purpose of this discussion we will consider B and BCa as the exogenously added buffer and S and SCa as the endogenous buffer, which for the moment is assumed to be non-mobile. The quantity j_{in} in eqn (5) is the flux of Ca^{2+} from the pipette (mainly that of BCa) and is given by (see eqn (4) of Mathias *et al.* (1990)):

$$j_{\text{in}} = ([\text{BCa}_p] - [\text{BCa}]) D_B \rho / R_p, \quad (6)$$

where R_p is the pipette resistance, ρ is the specific resistance of the pipette filling solution and D_B is the diffusion coefficient of the exogenous buffer (assumed to be the same in the Ca^{2+} -bound and -free form). The subscript P denotes pipette-related quantities.

The quantity j in eqn (5) is the flux across membranes (both across the plasma membrane and across storage organelles). For simplicity, this is assumed to be proportional to the deviation in $[Ca^{2+}]_i$ from a steady state value $[Ca^{2+}]_{i,\infty}$:

$$j = \gamma([Ca^{2+}]_i - [Ca^{2+}]_{i,\infty}) \quad (7)$$

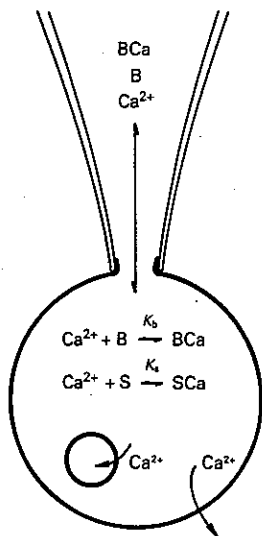


Fig. 3. Model used to analyse Ca²⁺ fluxes in a pipette-cell assembly. It is assumed that the indicator dye (B, free form; BCa, Ca²⁺-bound form) exchanges slowly by diffusion between pipette and cell. Inside the cell it competes with a fast, endogenous buffer S; calcium also is slowly removed by uptake mechanisms into intracellular stores and pumped across the plasma membrane (for details, see text).

where γ and $[Ca^{2+}]_{i,\infty}$ are constants reflecting the combined action of pumps, exchange carriers and membrane conductances. For the case of impulse-like depolarizations, and corresponding pulse-like influxes of calcium through voltage-activated channels, eqn (7) has to be extended:

$$j = \gamma([Ca^{2+}]_i - [Ca^{2+}]_{i,\infty}) - Ca_{inc} \delta(t - t_0) \quad (8)$$

where $\delta(t - t_0)$ is the delta function and Ca_{inc} is the integral calcium influx during the pulse.

In this analysis the cell is assumed to be in spatial equilibrium. This should be valid for times greater than 1 s, because spatial gradients dissipate within 100–500 ms in chromaffin cells of approximately 15 μ m diameter (see below). Combining eqns (5), (8) and (8) yields:

$$d[Ca^{2+}]_i/dt (1 + \kappa_B + \kappa_S) = \{D_B \rho / R_p \{ [BCa_p] - [Ca^{2+}]_i K_B [B_T] / (1 + [Ca^{2+}]_i K_B) \} + \gamma([Ca^{2+}]_{i,\infty} - [Ca^{2+}]_i) + Ca_{inc} \delta(t - t_0)\} / v \quad (9)$$

where the calcium binding capacities of B and S respectively have been introduced as

$$\kappa_B = d[BCa] / d[Ca^{2+}]_i \quad \text{and} \quad \kappa_S = d[SCa] / d[Ca^{2+}]_i \quad (10)$$

and $[BCa]$ has been replaced by its equilibrium value:

$$[BCa] = [Ca^{2+}]_i K_B [B_T] / (1 + [Ca^{2+}]_i K_B) \quad (11)$$

Here, $[B_T]$ is the total concentration of buffer B in the cell and K_B is its binding constant for calcium, while $[S_T]$ and K_S refer to the same parameters for buffer S. Combining eqns (10) and (11) we obtain:

$$\kappa_B = K_B [B_T] / (1 + [Ca^{2+}]_i K_B) \quad (12)$$

$[B_T]$ changes with time as buffer is dialysed into the cell. These changes in $[B_T]$ can be used to measure the impact of $[B_T]$ on cell buffering and deduce the relative contribution of endogenous Ca²⁺ buffers to the total amount of buffering within the cell. Below we describe two different approaches to estimating endogenous Ca²⁺ binding capacity; one based on the kinetic changes in the $[Ca^{2+}]_i$ signal produced by adding Fura-2 and a second based on the amount of Ca²⁺ bound to the added Fura-2.

Method 1 - Analysis of the kinetics of the Ca²⁺ signal. By analogy to eqns (5) and (6), the changes in Fura-2 concentration within the cell, $[B_T]$, occurring as the dye diffuses between pipette and cytoplasm can be described by a kinetic equation that reflects conservation of B:

$$d[B_T] / dt = ([B_{T,p}] - [B_T]) D_B \rho / (R_p v) \quad (13)$$

with $[B_{T,p}]$ the total concentration of B in the pipette. Here the simplifying assumption has been made that the diffusion coefficient of B is the same in the Ca²⁺-bound and -free forms. By this simplification, eqn (13) can be solved independently of eqn (9). Eqn (13) predicts that $[B_T]$ will exponentially approach $[B_{T,p}]$ with a loading time constant τ_L of:

$$\tau_L = v R_p / (D_B \rho) \quad (14)$$

This loading time constant can be measured when observing the fluorescence signal at 360 nm, the wavelength where Fura-2 fluorescence is independent of its Ca²⁺ binding state.

After $[B_T]$ has reached its maximum level, the only time-dependent quantity on the right-hand side of eqn (9) is $[Ca^{2+}]_i$. For small deviations from steady state, eqn (9) can be linearized with respect to $[Ca^{2+}]_i$, yielding exponential relaxations towards the steady state with the time constant, τ :

$$\tau = v \frac{(1 + \kappa_B + \kappa_S)}{\gamma + D_B \rho \kappa_B / R_p} \quad (15)$$

Equation (15) is best discussed in terms of a corrected time constant, τ' , which takes into account diffusion of buffer between cell and patch pipette. τ' is defined as:

$$\tau' = 1 / (\tau^{-1} - \tau_L^{-1}) \quad (16)$$

which, together with eqns (14) and (15), yields

$$\tau' = v \frac{1 + \kappa_B + \kappa_S}{\gamma - (1 + \kappa_B) D_B \rho / R_p} \quad (17)$$

This quantity is linear with respect to κ_B . Thus eqn (17) predicts a straight line if τ' values are plotted against κ_B . Experimentally, κ_B can be varied either by adding different amounts of Ca²⁺ buffer to the pipette or by varying $[Ca^{2+}]_i$ (eqn (12)). The negative x -axis intercept of such a plot is at $1 + \kappa_S$, yielding the endogenous Ca²⁺-binding capacity of the cell. It should be pointed out, however, that τ' depends critically on γ (the second term in the denominator of eqn (17) very often is only a small correction). γ , according to eqn (7), reflects the combined action of pumps and other calcium removal mechanisms, which may depend on $[Ca^{2+}]_i$, on the cell history, and on many other factors. Extrapolating such plots, therefore, may not be very reliable.

Method 2 - Analysis of the amount of Ca²⁺ bound to Fura-2. A more straightforward estimate of the endogenous binding capacity can be obtained by examining increments in $[BCa]$ during short pulses of Ca²⁺ influx. Integrating eqn (9) over the short period of influx yields:

$$\Delta[Ca^{2+}]_i + \Delta[BCa] + \Delta[SCa] = Ca_{inc} / v \quad (18)$$

where all but one term on the right side of eqn (9) have been neglected, assuming that the integration time is brief relative to τ , the time constant for the exponential removal of Ca²⁺ from the cell.

From eqn (10), small changes in $[Ca^{2+}]_i$ will produce the following changes in calcium bound to buffers:

$$\Delta[BCa] = \kappa_B \Delta[Ca^{2+}]_i \quad (19)$$

$$\Delta[SCa] = \kappa_S \Delta[Ca^{2+}]_i \quad (20)$$

where κ_B and κ_S are as defined in eqns (10) and (12). Incorporating these expressions into eqn (18), $\Delta[Ca^{2+}]_i$ then becomes:

$$\Delta[Ca^{2+}]_i v = Ca_{inc} / (1 + \kappa_B + \kappa_S) \quad (21)$$

By combining eqns (19) and (21), the change in the amount of calcium-bound form of Fura-2, $\Delta[BCa]v$, can be written as:

$$\Delta[BCa]v = Ca_{inc} \kappa_B / (1 + \kappa_B + \kappa_S) \quad (22)$$

This quantity is proportional to ΔF_{390} , the change in fluorescence at 390 nm. Ca_{inc} , on the other hand, is proportional to the integral of the calcium current (I_{Ca}) over the short pulse. Thus,

$$\Delta F_{390} = k \left(\int I_{Ca} dt \right) \left(\kappa_B / (1 + \kappa_B + \kappa_S) \right) \quad (23)$$

where k is a proportionality constant. Experimentally one can evaluate the quantity f :

$$f = \Delta F_{390} / \int I_{Ca} dt = k \kappa_B / (1 + \kappa_B + \kappa_S) \quad (24)$$

f has the physical meaning of the fraction of incoming calcium which is bound to Fura-2. A plot of f versus κ_B has the form of a binding isotherm and approaches a maximum value of f_{max} . A double reciprocal plot yields f_{max} and $1 + \kappa_S$ from the axis intercepts. With f_{max} known, eqn (24) can be rewritten:

$$f = f_{max} [\kappa_B / (1 + \kappa_S + \kappa_B)] \quad (25)$$

which can be rearranged to yield an expression for κ_S :

$$\kappa_S = \kappa_B (f_{max} - f) / f - 1 \quad (26)$$

Unlike eqn (17), eqn (26) is not restricted to cases where loading of exogenous buffer has approached equilibrium. Thus, several values of f can be conveniently measured while a cell is being loaded with Fura-2 and the binding capacity of the endogenous buffer, κ_B , can be determined from a given f value. This determination should be restricted to values of f well below f_{max} , to avoid problems caused in estimating f . For our analysis we used f values which were smaller than 0.75 f_{max} . Equation (26) as derived here is, however, restricted to small changes in $[Ca^{2+}]_i$, because of the approximation in eqns (19) and (20). This can be generalized by noting explicitly that (see eqn (11)):

$$\Delta[BCa] = [BCa]_2 - [BCa]_1 \quad (27)$$

$$= K_B B_T \left\{ \frac{[Ca^{2+}]_2}{1 + [Ca^{2+}]_2 K_B} - \frac{[Ca^{2+}]_1}{1 + [Ca^{2+}]_1 K_B} \right\} \quad (28)$$

$$= K_B B_T \frac{[Ca^{2+}]_2 - [Ca^{2+}]_1}{(1 + [Ca^{2+}]_2 K_B)(1 + [Ca^{2+}]_1 K_B)} \quad (29)$$

where the subscript 2 refers to values following the voltage pulse depolarization, whereas subscript 1 refers to those before the depolarization. Equation (19) can therefore be written:

$$\Delta[BCa] = \kappa'_B \Delta[Ca^{2+}]_i \quad (30)$$

with

$$\kappa'_B = B_T K_B / [(1 + [Ca^{2+}]_2 K_B)(1 + [Ca^{2+}]_1 K_B)] \quad (31)$$

It is seen that the quantity κ'_B is identical to κ_B for small changes in $[Ca^{2+}]_i$. It can be used to replace κ_B in the derivation of eqns (21) to (26), leading to:

$$\kappa_S = \kappa'_B (f_{max} - f) / f - 1 \quad (32)$$

In the following we use eqn (32) instead of eqn (26) whenever changes in $[Ca^{2+}]_i$ cannot be considered small.

Measurement of fluorescence decrements and calcium current integrals

The ratio f , as defined in eqn (24), requires measurement of two parameters during depolarizing pulses: the fluorescence decrement at 390 nm and the Ca^{2+} current integral. For this purpose fluorescence at both 360 and 390 nm was sampled every 500 ms as described in the companion paper (Augustine & Neher, 1992). Linear regression was used to fit straight lines to segments of the 390 nm trace (each 4-10 sample points in length) both before and immediately following depolarizing pulses. Both lines were extrapolated to the time of the stimulus, and the difference between the two values was taken as the fluorescence decrement.

Ca^{2+} currents in response to depolarizing stimuli were measured, employing a P/4-technique (Armstrong & Bezanilla, 1977). In some cases there were residual Na^+ currents not eliminated by the TTX in the external saline (see Fig. 7 for a worst-case example). In these cases Ca^{2+} current integral was estimated as the product of the plateau inward current and the length of the depolarizing pulse.

Determination of K_B , the binding constant of Fura-2

Both methods for determining κ_S require calculation of κ_B which in turn relies on knowledge of K_B , the calcium binding constant of Fura-2 in this case. Dual excitation-wavelength ratio measurements of Fura-2 are usually calibrated by measuring three constants: K'_D , an 'apparent' calcium dissociation constant for Fura-2, R_{min} , the limiting fluorescence ratio at low calcium concentrations, and R_{max} , the limiting ratio at high calcium concentrations (Grynkiewicz *et al.* 1985). These three calibration constants can be used to determine K_B , if one of the excitation wavelengths used to measure R is at the isostilbic point for Fura-2, as described below.

K'_D , the effective calcium dissociation constant for Fura-2, was already defined in eqn (4) in terms of fluorescence parameters measured at a single calcium-sensitive wavelength [$K'_D = K_D (F_{max}/F_{min})$]. When the other excitation wavelength is at the isostilbic point (~ 360 nm), then the fluorescence intensities of the free and bound forms of Fura-2, F_{360} , are equal. Multiplying both the numerator and denominator of eqn (4) by this value yields:

$$K'_D = K_D \left(\frac{F_{max}/F_{360}}{F_{min}/F_{360}} \right) \quad (33)$$

Because $R_{min} = F_{360}/F_{max}$ and $R_{max} = F_{360}/F_{min}$, then

$$K'_D = K_D (R_{max}/R_{min}) \quad (34)$$

and K_B , the inverse of K'_D , is:

$$K_B = R_{max} / (R_{min} K'_D) \quad (35)$$

Thus, the calcium binding constant of Fura-2 in cytoplasm can readily be calculated from the three constants routinely determined during calibration of dual-wavelength ratio measurements.

The numerical value of f_{max}

Estimation of κ_S as in Method 2 also requires determination of f_{max} , the fraction of incoming calcium captured by Fura-2 at saturating concentrations. Whereas only relative numbers, f/f_{max} , are required for evaluation of κ_S , it is also important to know whether the absolute value of f_{max} is compatible with the expectation that, at high dye concentration, Fura-2 should capture all of the calcium entering the cell. If S_{f2} , S_{b2} , S_{f1} and S_{b1} are specific fluorescence intensities for the free (f subscript) and bound (b subscript) forms of Fura-2 measured at excitation wavelengths 2 and 1, as defined by Grynkiewicz *et al.* (1985), then R_{min} and R_{max} are given by S_{f1}/S_{b1} and S_{f2}/S_{b2} , respectively. When excitation wavelength 1 is at the isostilbic point, a simple relationship can be obtained between the relative fluorescence change during a stimulus ($\Delta F_{390}/F_{360}$) and the integral of the calcium current. In this case, the ratio $\Delta F_{390}/F_{360}$ is:

$$\frac{\Delta F_{390}}{F_{360}} = \frac{\Delta[BCa] (S_{b2} - S_{f2})}{[B_T] S_{b1}} = \frac{\Delta[BCa]}{[B_T]} (R_{max}^{-1} - R_{min}^{-1}), \quad (36)$$

where use again has been made of $S_{b1} = S_{f1}$.

If the concentration of Fura-2 is sufficiently high, then all of the Ca^{2+} -influx will be taken up by Fura-2 and $\Delta[\text{BCa}]$ will be proportional to the calcium current integral according to:

$$\Delta[\text{BCa}] = \int -I_{\text{Ca}} dt / (2FV) \quad (37)$$

where F is the Faraday constant and V is the cell volume. Thus, the value of the ratio f_{max} (eqns (24) and (25)) should be given by:

$$f_{\text{max}} = \frac{\Delta F_{390}}{\int I_{\text{Ca}} dt} = \frac{F_{390}(R_{\text{min}} - R_{\text{max}})}{2FV[\text{B}_T]R_{\text{min}}R_{\text{max}}} \quad (38)$$

Here, F_{390} and ΔF_{390} should be measured in the same (but otherwise arbitrary) units, v is the accessible volume of the cell and $[\text{B}_T]$, after complete loading, is assumed to be equal to the Fura-2 concentration in the pipette.

RESULTS

We first use digital imaging methods to examine spatial gradients of $[\text{Ca}^{2+}]_i$ during depolarization and then examine the properties of the intrinsic buffers that influence the depolarization-induced $[\text{Ca}^{2+}]_i$ signal. In the Discussion we evaluate the impact of these buffers, as well as of the Fura-2 added to the cytoplasm, on the $[\text{Ca}^{2+}]_i$ signal produced by depolarization.

Imaging spatial gradients of Ca^{2+}

Video imaging allowed us to visualize $[\text{Ca}^{2+}]_i$ gradients within single chromaffin cells. In these experiments, the microscope was focused on the central plane of the spherical (or cylindrical) cell, to attempt to measure $[\text{Ca}^{2+}]_i$ changes with minimal contributions from the top and bottom regions of the cell. Although the optical sectioning properties of the microscope were not ideal (Hiraoka *et al.* 1990), fluorescence signals were different at different levels of focus within the depth of the cell. This indicates that the fluorescence signals measured in central focal planes should have reduced contributions from the other, out of focus, regions of the cell.

The resting fluorescence of Fura-2 was often brightest in the central region of the cell (e.g. Fig. 1A). Although some of this non-uniformity was probably due to the spherical geometry of the cell, it often appeared that the nucleus was more fluorescent than the cell cytoplasm. Accumulation of fluorescent Ca^{2+} indicators in the nuclear region has been found for other cells (e.g. Hernandez-Cruz *et al.* 1990) and could be caused by nuclear accumulation of dye or exclusion of dye from the non-nuclear portion of the cytoplasm (for example, by dye being excluded by chromaffin granules). Because the ratio of fluorescence emitted when cells were alternatively excited by 360 and 390 nm was constant throughout the cell (not shown), these gradients do not represent differences in $[\text{Ca}^{2+}]_i$ within the nucleus, as has been reported for other cells (Williams, Fogarty, Tsien & Fay, 1985; Hernandez-Cruz *et al.* 1990). Whatever the cause of this non-uniformity, it is expected that it would not distort the measurements of $[\text{Ca}^{2+}]_i$, because of the use of the ratio method. The spatial uniformity of the resting $[\text{Ca}^{2+}]_i$ signal indicates that this is the case.

Depolarization caused an influx of Ca^{2+} , as measured by a transient Ca^{2+} current (Fenwick *et al.* 1982; Clapham & Neher, 1984; Hoshi, Rothlein & Smith, 1984; Kim & Neher, 1987; Augustine & Neher, 1992), and a rise in $[\text{Ca}^{2+}]_i$ (Knight & Kesteven, 1983; O'Sullivan *et al.* 1989; Augustine & Neher, 1992). Examples of $[\text{Ca}^{2+}]_i$ signals

produced by 500-ms-long depolarization to +5 mV are shown in Fig. 4. At the beginning of the depolarization, the changes in Fura-2 fluorescence were restricted to the edge of the cell (Fig. 4A). At later time during the depolarization, these changes were present throughout the cell but still usually were largest near the membrane

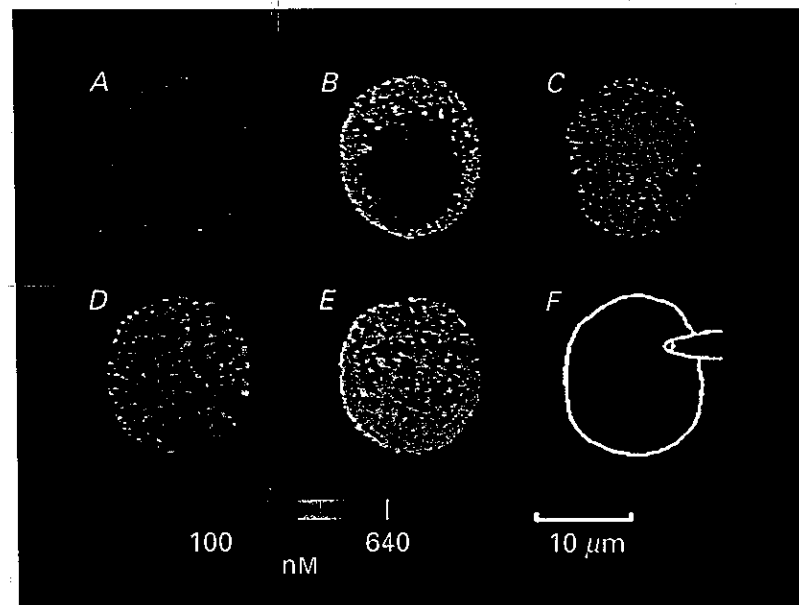


Fig. 4. Imaging of $[\text{Ca}^{2+}]_i$ changes in a single chromaffin cell responding to a 500-ms-long depolarization to +5 mV. Changes in relative fluorescence intensity (390 nm excitation) have been encoded into the pseudocolor scale shown at the lower left. A-C, images obtained during the depolarization, at 100 ms, 300 ms and 500 ms after the beginning of the depolarization respectively. D and E, fluorescence maps at 1 and 10 s following the end of the depolarization. F, schematic illustration showing the position of the patch pipette relative to the outline of the cell. During the experiment the microscope was focused on a plane through the centre of the cell and the fluorescence of the patch pipette was not visible.

(Fig. 4B and C). Repolarization of the membrane potential rapidly deactivated the Ca^{2+} current and stopped Ca^{2+} entry into the cell; this caused a loss of the fluorescence gradients within the cell (Fig. 4D) and, at later times, the changes in fluorescence gradually subsided in a spatially uniform fashion (Fig. 4E). Several observations indicate that these changes in fluorescence were due to $[\text{Ca}^{2+}]_i$ gradients resulting from Ca^{2+} entry into the cell. The magnitudes of the changes were closely correlated with the size of the voltage-dependent Ca^{2+} current, both signals being very small during depolarizations to potentials more negative than -10 mV or more positive than +60 mV (not shown). These signals also were absent in two cells dialysed with a high concentration of the Ca^{2+} buffer, EGTA (10 mM, rather than the

usual 0.5 mM). Finally, the changes in fluorescence were very small when the Fura-2 was excited at 360 nm, its isostilbic (Ca^{2+} independent) wavelength (Grynkiewicz *et al.* 1985). It therefore appears that these images are a consequence of radial gradients in $[\text{Ca}^{2+}]_i$ that produce a similar distribution of Ca^{2+} -bound Fura-2. Similar

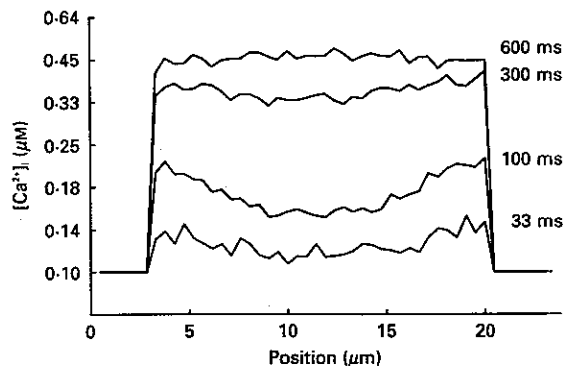


Fig. 5. Spatial distribution of depolarization-induced changes in Fura-2 fluorescence. The cell was depolarized to +5 mV for 500 ms. Fluorescence changes were measured along a line perpendicular to the axis of the patch pipette at various times during (33, 100 and 300 ms traces) and 100 ms following (600 ms trace) the depolarization.

gradients have been reported previously in depolarized chromaffin cells (O'Sullivan *et al.* 1989) and frog neurones (Lipscombe, Madison, Poenie, Reuter, Tsien & Tsien, 1988; Hernandez-Cruz *et al.* 1990).

Spatial profiles of the changes in $[\text{Ca}^{2+}]_i$ induced by depolarization of another cell are shown in the linescans of Fig. 5. The concave, inwardly directed gradients of $[\text{Ca}^{2+}]_i$ were evident throughout the depolarization (33, 100 and 300 ms curves), but rapidly dissipated following the depolarization (600 ms curve). Similar gradients were seen in each of the sixteen cells successfully examined, although the specific shape of the profiles (steepness and symmetry of the gradients) varied from cell to cell. This variability may have been due to geometrical differences between recordings, such as the position of the focal plane relative to the top and bottom of the cell. Qualitatively similar gradients were seen in cells dialysed with concentrations of Fura-2 ranging from 0.1–0.5 mM. However, the magnitudes of the $[\text{Ca}^{2+}]_i$ changes were smaller at the higher concentrations of the dye, due to the buffering effects of Fura-2 on $[\text{Ca}^{2+}]_i$ changes (see below).

The time course of the $[\text{Ca}^{2+}]_i$ signals depended upon the location within the cell (Fig. 6). $[\text{Ca}^{2+}]_i$ signals near the edge of the cell rose rapidly and began to reach a maximum as the Ca^{2+} current inactivated. $[\text{Ca}^{2+}]_i$ signals in the centre of the cell were delayed relative to those at the periphery, but still reached the same maximum after the Ca^{2+} current ceased. The time required for spatial equilibration was rapid, probably more rapid than the time resolution of the video camera (*ca* 100 ms; see Methods). At all locations, $[\text{Ca}^{2+}]_i$ remained high for several seconds, gradually declining in a monotonic fashion (see also Fig. 7, as well as O'Sullivan *et al.* 1989;

Augustine & Neher, 1992). In these experiments we saw no indication of the large and localized release of Ca^{2+} from internal stores reported in intact chromaffin cells depolarized with high external K^+ or acetylcholine (O'Sullivan *et al.* 1989).

Endogenous buffers of the chromaffin cell

The characteristics of the fluorescence changes described above reflect the influence of both endogenous buffers and those added by the pipette (Fura-2 and

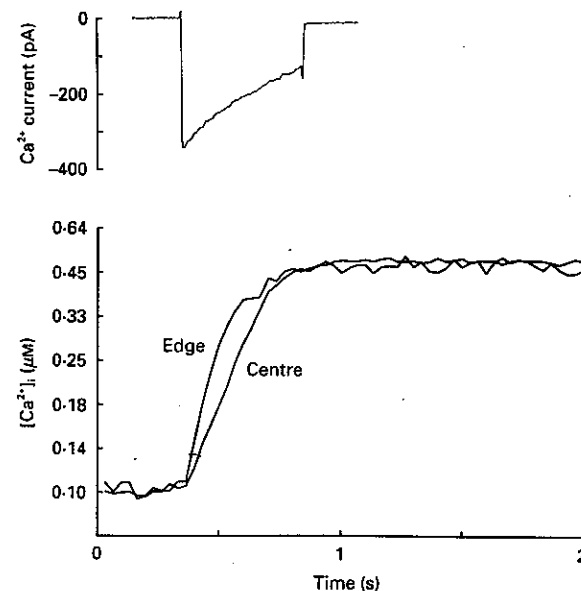


Fig. 6. Time course of Ca^{2+} influx and $[\text{Ca}^{2+}]_i$ changes in a depolarized chromaffin cell. Top, Ca^{2+} current elicited by a 500-ms-long depolarization to +5 mV from a holding potential of -79 mV. Bottom, simultaneous measurements of fluorescence changes within small regions near the edge and centre of the cell. Same experiment as in Fig. 5.

EGTA). In order to reveal the true characteristics of the $[\text{Ca}^{2+}]_i$ signal resulting from depolarization it is necessary to define the contribution of endogenous and exogenous buffers to the measured fluorescence changes. While the buffering properties of exogenous Ca^{2+} buffers (κ_B in eqn (10)) are readily definable, little is known about the properties of the endogenous buffers (κ_S in eqn (10)). In this section we use spatially averaged, photomultiplier measurements of Fura-2 fluorescence intensities at two wavelengths to deduce several properties of the endogenous buffers.

Two approaches for estimating cytoplasmic Ca^{2+} -binding capacity were presented in the Methods section. Both rely on a kinetic separation between fast buffering mechanisms and slower removal mechanisms. Furthermore they assume spatial uniformity of $[\text{Ca}^{2+}]_i$ at early times following a depolarizing pulse, such that fluorescence readings can be taken before calcium is removed. Figure 6 shows that

$[Ca^{2+}]_i$ is uniform at the end of a long depolarizing pulse and that removal is, indeed, slow with respect to the time scale of spatial re-equilibration within the cell. Figure 7 further demonstrates the kinetic separation with a spatially averaged Fura-2 signal recorded from a chromaffin cell by means of a photomultiplier. Figure 7A shows the

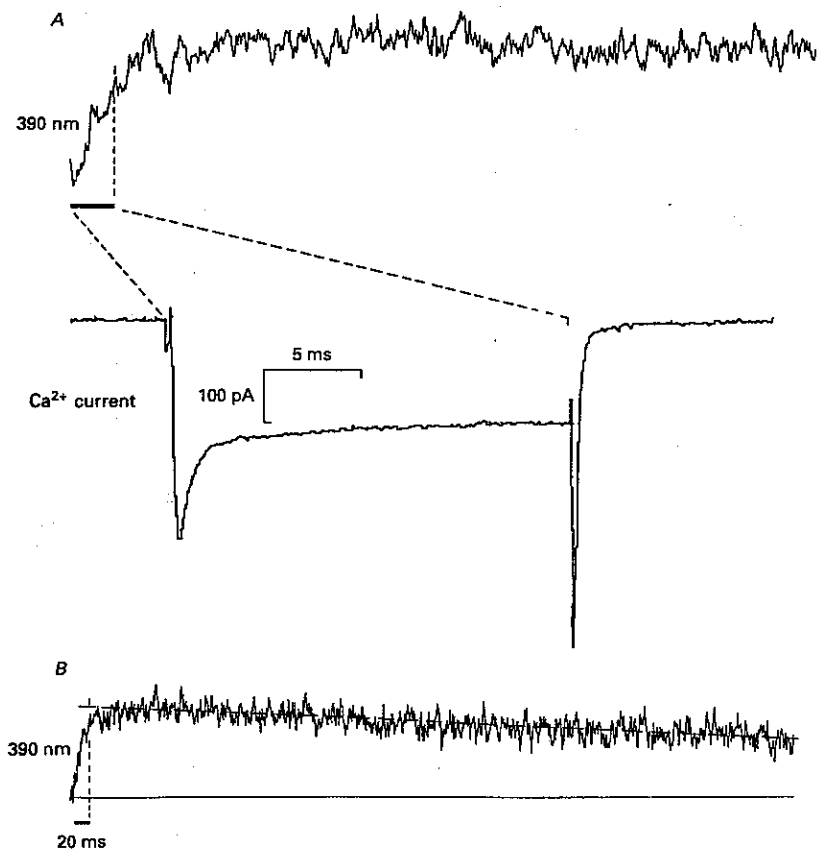


Fig. 7. Ca^{2+} current and Fura-2 fluorescence (390 nm) during a 20 ms depolarizing pulse to +10 mV ($V_{hold} = -70$ mV). The pipette contained standard internal dialysis solution plus 50 μM -K-Fura-2 and 20 μM -EGTA. External Ca^{2+} concentration was 1 mM. The fluorescence traces are averages (inverted polarity!) from twelve individual pulses. The horizontal bar (in A) indicates the stimulation interval of 20 ms duration. This is expanded in the current trace below. B, same signal as fluorescence trace of A on a compressed time scale. The dashed line was drawn by eye to emphasize the linearity of the return to baseline.

changes in fluorescence (390 nm excitation wavelength) produced by a depolarizing stimulus of 20 ms duration. In this figure, fluorescence is displayed with negative scaling, so that an upward deflection represents a decrease in fluorescence and an

increase $[Ca^{2+}]_i$. The depolarizing stimulus elicited the Ca^{2+} current illustrated in the expanded section. $[Ca^{2+}]_i$ increased during the stimulus, and for 10 to 20 ms following the stimulus. The increase that follows the stimulus may either reflect Fura-2 binding kinetics or spatial redistribution within the cell. Similar delayed increases have been described in *Aplysia* neurones (Tillotson & Nasai, 1988) and rat sympathetic neurones (Thayer & Miller, 1990). In these cells the delays are longer than in chromaffin cells, presumably because the larger diameters of these cells increases the time required for spatial re-equilibration. After the delayed increase, the fluorescence signal slowly decayed back to the resting $[Ca^{2+}]_i$ level over a period of 10–30 s. Similar gradual returns to baseline $[Ca^{2+}]_i$ have been seen in many cell types following depolarization (e.g. Gorman & Thomas, 1978; Smith & Zucker, 1980; McBurney & Neering 1985; Ahmed & Connor, 1988; Thayer & Miller, 1990) and presumably reflect the slow removal of Ca^{2+} from the cytoplasm. Analysing the rate of this slow decline as a function of added calcium buffer was used in Method 1 to estimate cytoplasmic Ca^{2+} -binding capacity.

Figure 7B shows the same Fura-2 signal as in A, but on a more compressed time scale. A straight line has been fitted by eye to part of the record in order to show that the decay is linear on such a time scale, although this decay actually represents the start of a more or less exponential return to baseline. The important point is that there is no indication of additional kinetic components, indicative of buffering or removal mechanisms of intermediate components. This warrants the simple model of Fig. 3. It also illustrates that the amplitude of the depolarization-induced increment in fluorescence can be conveniently measured by extrapolating the slow relaxation back to the time of the stimulus, and comparing this to the pre-stimulus baseline. Such a measurement was necessary for Method 2, the second means of estimating cytoplasmic Ca^{2+} -binding capacity.

Capacity of the endogenous Ca^{2+} buffer

In both procedures used for estimating the cytoplasmic Ca^{2+} buffer capacity, κ_s , Fura-2 is the only exogenous calcium buffer and is loaded into the cell by dialysis from a patch pipette. Figure 8A illustrates an experiment where a relatively thin-tipped pipette was used to slowly deliver Fura-2 to the cytoplasm of a chromaffin cell. A high concentration of Fura-2 (0.4 mM) was used in this experiment to deliberately emphasize the Ca^{2+} -buffering effects of Fura-2. The uppermost trace represents fluorescence at 360 nm. It displays the loading time course of Fura-2 and was well fitted by an exponential with a time constant of 190 s. The centre trace is fluorescence at 390 nm, which shows step-like decrements whenever depolarizing stimuli (to +10 mV test potential from a holding potential of -70 mV) were given. The bottom trace in Fig. 8A displays $[Ca^{2+}]_i$ as calculated from the fluorescence ratio (Grynkiewicz *et al.* 1985). The amplitudes of the depolarization-induced changes in $[Ca^{2+}]_i$ decreased as Fura-2 diffused into the cell. This reflects the buffering effect of the added Fura-2, which progressively takes up a higher proportion of the incoming calcium. At the same time, recovery of the $[Ca^{2+}]_i$ changes became slower, which is also due to the buffer capacity added by Fura-2 (eqn 15).

Both procedures used to estimate κ_s also require knowledge of κ_b , the Ca^{2+} -binding capacity of the Fura-2 added to the cytoplasm of a cell. This was calculated from

$[B_T]$, the cellular concentration of total Fura-2, and K_B , the Ca^{2+} -binding constant of Fura-2 in the cellular environment (eqn (12)). $[B_T]$ was estimated from the 360 nm fluorescence signal, assuming that the steady state level of the 360 nm signal represents fully equilibrated Fura-2 concentration ($400 \mu M$ in the case of the

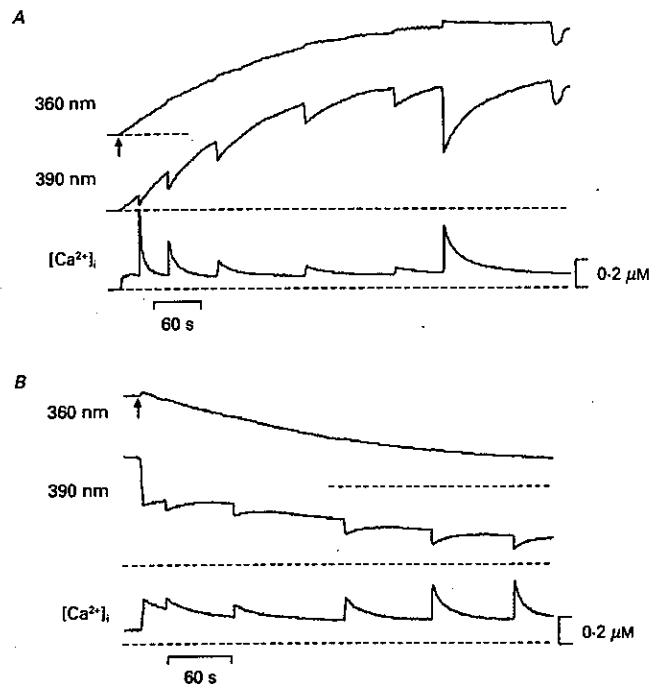


Fig. 8. Loading and unloading a chromaffin cell with Fura-2. *A*, a whole-cell configuration was achieved at the time of the arrow with a pipette containing standard filling solution plus $400 \mu M$ -K-Fura-2 (no EGTA). Six depolarizing pulses to $+10$ mV were given at irregular intervals from a holding potential of -70 mV; pulses one to five were 50 ms in duration, pulse six was 200 ms. The depression in the fluorescence traces towards the end marks the time when the pipette was slowly removed, leaving behind an intact cell. *B*, a few minutes later a second whole-cell recording was achieved on the same cell (arrow) with a pipette containing standard filling solution plus $50 \mu M$ -K-Fura-2. Traces are arranged as in *A*. Five depolarizing pulses of 20 ms duration were given while Fura-2 slowly diffused out of the cell. Extracellular Ca^{2+} concentration was 5 mM.

experiment of Fig. 8*A*). K_B was calculated from the Fura-2 calibration constants (eqn (35)) and was $6.6 \times 10^8 M^{-1}$.

Estimate based on the time constant of $[Ca^{2+}]_i$ signals

The theory presented above indicates that the endogenous Ca^{2+} -binding capacity of the chromaffin cell can be estimated from the time constants of recovery of $[Ca^{2+}]_i$ after small perturbations (Method 1). Intuitively this can be understood by

considering that, for a given increment in $[Ca^{2+}]_i$, the load of calcium to be removed from the cell is increased with added binding capacity. There are a number of limitations to such an approach. First, the time constants depend on numerous cellular parameters (eqn (17)), particularly those relating to the poorly defined slow

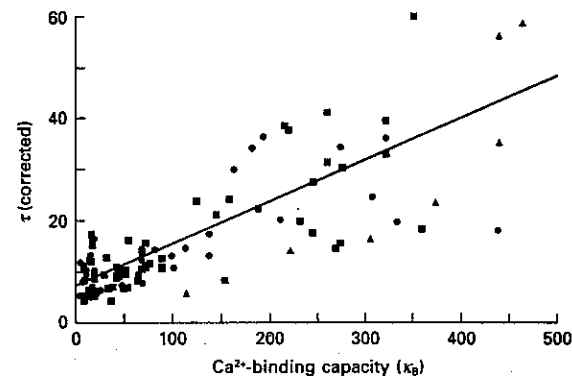


Fig. 9. Time constants of recovery of the depolarization-induced calcium increase vary with the calcium-binding capacity of added Fura-2 (no extra EGTA added). Time constants were evaluated from exponential fits to recovery time courses. For larger excursions, where deviations from the exponential time course were evident, the fit was restricted to the final approach towards the long-term baseline. Data from three groups of cells with different amounts of added Fura-2 have been pooled. Experiments on the first group (\bullet) were performed at 5 mM external calcium concentration, the second group (\blacksquare) had 2 mM external calcium, and the third one (\blacktriangle) again with 5 mM external calcium. Calcium-binding capacity (κ_B) was calculated according to eqn (12), with B_T estimated from the fluorescence intensity at 360 nm at the time of the stimulus, and $[Ca^{2+}]_i$ being taken as that of the steady-state baseline. The straight line is a linear regression fit to all data points.

mechanisms for Ca^{2+} removal. Second, the estimate should apply only to small deviations from equilibrium (small with respect to the dissociation constant of Fura-2), whereas experimentally induced deviations usually were substantial to provide adequate resolution for measurement. Finally, the analysis should strictly apply only to the steady state, after the loading process has come to completion.

Despite these limitations, exponentials could be fitted to the decay of many $[Ca^{2+}]_i$ signals (see also Thayer & Miller, 1990). As evident in Fig. 8*A*, the time course of decay became slower as the intracellular concentration of Fura-2 was elevated. Figure 9 presents a plot of τ' , as defined by eqn (16), versus κ_B , the Ca^{2+} -binding capacity of intracellular Fura-2. According to eqn (17), τ' should increase linearly with κ_B . In this figure the data from eighteen experiments, including values obtained at steady state and others measured during slow increases in Fura-2 concentration, are used. Values at any binding capacity scatter by about a factor of 2 to 3 in different cells. However, a clear trend is apparent in the data and a linear regression fitted to all data points yielded a negative x-intercept of 89, which is an estimate of κ_S , the Ca^{2+} -binding capacity of the endogenous buffer (eqn (17)). This indicates that

in the absence of Fura-2, only 1/90 of the calcium entering the cell appears as free calcium. The y -intercept of Fig. 9 indicates the recovery time constant expected in the absence of Fura-2. The range of values encountered was 5–12 s in different experiments, with a value of 7.2 s derived from a linear regression fit to all points.

Estimate based on the fraction of calcium bound by Fura-2

Method 2 is based on analysing the amplitudes of fluorescence changes which occur during depolarizing stimuli. While changes in $[Ca^{2+}]_i$, as measured by fluorescence ratios, decrease during loading of a cell with excess amounts of Fura-2, the fraction of calcium entering that is captured by Fura-2 increases because Fura-2 competes more favourably with the endogenous buffer. It was shown above that the fraction f , defined as the ratio of ΔF_{390} over the calcium current integral, should increase monotonically with an increasing concentration of Fura-2. It reaches a limiting value, f_{max} , when all of the incoming calcium is taken up by Fura-2. In this case, ΔF_{390} is an accurate measure of Ca^{2+} flux. In the example of Fig. 8A, six depolarizing stimuli were given while Fura-2 diffused into the cell. The first five pulses were each 50 ms in duration. They resulted in progressively larger f -values, as shown in Fig. 10C, where they are plotted as \bullet . The rightmost round symbol in Fig. 10C represents the sixth response of Fig. 8A, which was elicited by a 200-ms-long pulse. Its Ca^{2+} current integral was 3.60 times larger than that of the preceding pulse and the magnitude of the resulting fluorescence decrement was larger by the same factor (within 2%), such that f -values were almost identical. This sequence of responses illustrates both expectations of the theory: (i) f eventually reaches a maximum during Fura-2 loading and, (ii) once at this maximum, the fluorescence signal is proportional to the amount of Ca^{2+} entry.

The relationship between f and κ_B is shown for two different cells in Fig. 10A and C. Both sets of data illustrate the saturation of f as a function of κ_B that was predicted from theory (eqn (25)). Figures 10B and D are double reciprocal plots of data in A and C, respectively. Close inspection reveals that there is some upwards curvature in the plots. This is a consistent trend in all the cells analysed this way ($n = 6$). In order to obtain estimates for f_{max} , straight lines were fitted to the double reciprocal plots, restricting the regression range to nine values closest to the y -axis. These fits are shown in Fig. 10B and D. Between cells, f_{max} varied with a relative standard deviation of 10%. κ_S was estimated according to eqns (26) or (32) (see Methods section). The mean value (\pm s.e.m.) from nine individual measurements originating from six different cells was 75 ± 7 . This value is definitely more accurate than the one derived through Method 1. It means that, in the absence of Fura-2, out of seventy-six parts of calcium entering the cell, seventy-five parts are bound to endogenous buffer and one part appears as free calcium.

Once f_{max} has been determined on a set-up, the integral Ca^{2+} -flux can be determined by inversion of eqn (24):

$$\int I_{Ca} dt = \Delta F_{390}/f_{max} \quad (39)$$

provided that the concentration of Fura-2 is high enough to achieve saturating levels of κ_B . In evaluating eqn (39) it is important to note that the physical units of ΔF_{390}

should be the same as those used during determination of f_{max} . Also, photomultiplier sensitivity and illumination conditions have to be absolutely constant. Some of these influences can be eliminated by relating all fluorescence values to a fluorescence standard. In this context, fluorescent beads (Fluoresbrite TM Carboxylate BB beads

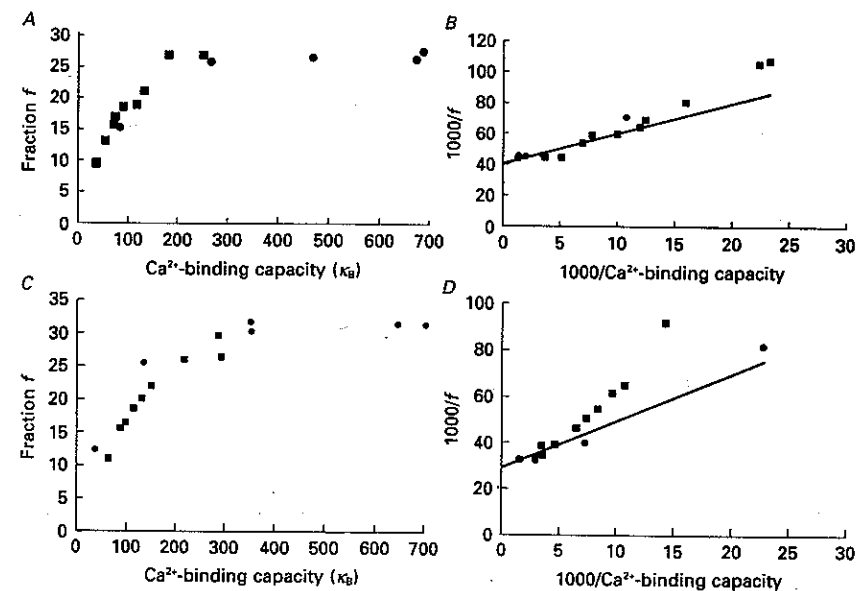


Fig. 10. The 'fraction f ', the ratio of ΔF_{390} over calcium current integral, as a function of calcium-binding capacity of Fura-2 (κ_B) during loading (\bullet) and unloading (\blacksquare). ΔF_{390} is the difference in fluorescence readings at 390 nm before and after a stimulus (see Methods section). A and C, two different experiments similar to those of Fig. 8. B and D, double reciprocal plots of the data in A and C, respectively. The units on the ordinate are fluorescence units/Coulombs. No dimensions are given because fluorescence units are arbitrary. Ca^{2+} -binding capacity of Fura-2 was estimated according to eqn (31). Straight lines in B and D are linear regression fits, restricted to nine data points closest to the ordinate.

4.3 μ m diameter, from Polyscience, Northampton, UK) proved very convenient because they have fluorescence intensities similar to chromaffin cells under the conditions of our measurement. Beads were added to the chamber at low density such that their fluorescence readings could be taken in between measurements or cells.

After a cell has been loaded to the extent that all of the incoming calcium is taken up by Fura-2, the magnitude of depolarization-induced fluorescence changes should be directly proportional to the integral of calcium currents. Equation (38), in theory would allow the calculation of the proportionality constant. This equation assumes that the dye has equilibrated diffusionally, such that the total Fura-2 concentration (B_T) is the same as in the pipette. In addition, this calculation requires the

calibration constants R_{\min} and R_{\max} , measurement of absolute fluorescence F_{360} , and of cell volume. Most of these parameters are known quite accurately. Cell volume, however, presents a problem, since only volume accessible to Fura-2 should actually be considered. Since this was not known, we used eqn (38) to calculate accessible volume from measured f_{\max} values. We also determined total cell volume by measuring cell diameter and assuming that the cells were perfect spheres. By dividing accessible volume by total volume, an accessible volume fraction can be calculated. In six measurements of this kind, a value of 0.85 ± 0.09 (mean \pm s.e.m.) was found. It thus appears that about 15% of the volume of the cell excludes dye. It should be stressed that this is only an order-of-magnitude estimate because of the many assumptions involved. The fact that the value is reasonable, on the other hand, shows the internal consistency of all the assumptions made and indicates that fluorescence changes under these conditions do indeed reflect the calcium entering the cell, as opposed to calcium released from intracellular stores.

Mobility of the endogenous Ca^{2+} buffer

If the endogenous buffer is diffusible, it will be lost from the cell as it is washed out of the cytoplasm and diluted by the much larger volume of the patch pipette. In principle, this could be tested by evaluating κ_s , the endogenous calcium-binding capacity (eqn (26)), at different times following patch rupture. However, the estimate of κ_s based on f -values requires accurate determination of f_{\max} . This is only possible when f approaches f_{\max} , which normally takes place after about 1 min of loading. Under these conditions, however, small errors in f lead to larger errors in determining κ_s , as implied by the specific form of eqn (26). Therefore κ_B has to be reduced again, if κ_B is to be measured at later times.

To achieve this, we sequentially loaded and unloaded cells using two pipettes. Figures 8A and B present such an experiment. The artifact in the fluorescence traces, near the end of the recording in Fig. 8A, marks the time when the first pipette was slowly removed from the cell. Three minutes later another whole-cell recording was established on the same cell, using a second pipette. The new pipette was filled with only $50 \mu\text{M}$ -Fura-2, as opposed to $400 \mu\text{M}$ for the case of the first pipette. The recordings of Fig. 8B shows the ensuing fluorescence signals. The fluorescence at 360 nm slowly returned to low levels, as Fura-2 concentration in the cell decreased. $[\text{Ca}^{2+}]_i$ started out relatively high because the cell was slightly damaged during breakthrough with the second pipette. However, changes in the fluorescence signal due to voltage pulses could still be well resolved. Depolarization-induced increments in $[\text{Ca}^{2+}]_i$ increased, and the time constants of recovery shortened, as Fura-2 diffused out of the cell. An analysis of f -values was performed; the corresponding data points are plotted in Fig. 10C as square symbols, while circles indicate measurements made during Fura-2 loading. Both sets of data points are quite well described by the same curve. Correspondingly, determination of κ_s on four cells (according to eqn (26)) gave similar mean values for loading and unloading runs, as shown in Table 1. Although there is substantial scatter in the values, it is clear that there is no tendency for κ_s to decrease during the 10–15 min duration of the whole-cell recording. Thus, it appears that most of the endogenous cytoplasmic Ca^{2+} buffer is not mobile.

TABLE 1. Endogenous calcium binding capacities according to eqn (24) during loading and unloading of Fura-2

κ_s -loading	Loading time constant (s)	Dialysis time (s)	κ_s -unloading	Unloading time constant (s)
93	120	670	78 ± 12 (8)	171
63 ± 21 (2)	192	690	110 ± 72 (6)	190
52	74	906	69 ± 28 (9)	235

Each line represents one cell; values given are means \pm s.d. (n) of those data points where f was smaller than f_{\max} by at least 20%. Dialysis time is the total time for which the cell had been in contact, with a patch pipette up to the mean time of the unloading measurement.

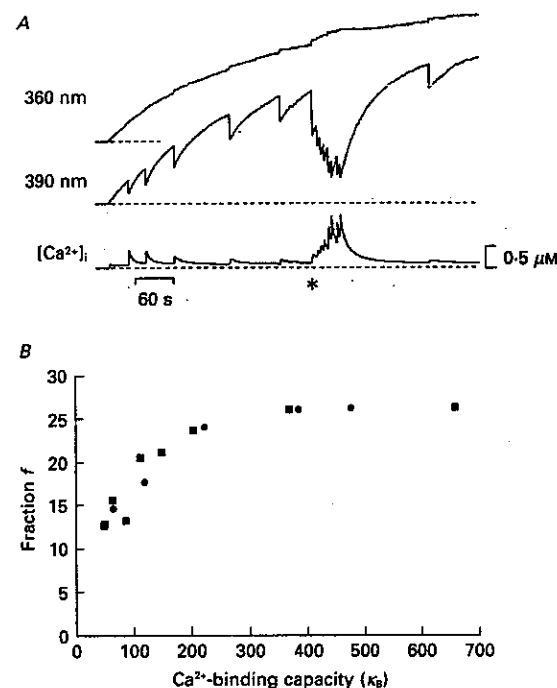


Fig. 11. Effect of high $[\text{Ca}^{2+}]_i$ on the calcium-binding capacity of Fura-2. A is an experiment very similar to that of Fig. 8, except that at the time of the asterisk a rapid train of depolarizing stimuli was given, which increased $[\text{Ca}^{2+}]_i$ to almost $1 \mu\text{M}$. The 'fraction f ' was calculated and plotted in B both during the loading process (●) and for individual stimuli during or after the pulse train (■) as in Fig. 10.

Saturability of the endogenous buffer

$[Ca^{2+}]_i$ often varied between 0.2 and 0.5 μM as a result of the manipulations performed in some experiments (e.g. Fig. 8B). If the endogenous Ca^{2+} buffer changes its degree of saturation during such changes in $[Ca^{2+}]_i$, then κ_s would also change. For example, if the endogenous buffer had the same affinity as Fura-2, then κ_s would change 3- to 4-fold over this range of $[Ca^{2+}]_i$ (eqn (12)). Thus, changes in $[Ca^{2+}]_i$ can be used to provide some information on the degree of saturation of the endogenous buffer.

$[Ca^{2+}]_i$ can readily be changed during an experiment by giving trains of depolarizations, as illustrated in Fig. 11A. Initially five well-separated depolarizations were applied to determine values of f and f_{max} at relatively low $[Ca^{2+}]_i$ (0.16–0.22 μM). These were followed by a rapid train of pulses that increased $[Ca^{2+}]_i$ to a mean value of 0.71 μM . Figure 11B demonstrates that values of f obtained at low $[Ca^{2+}]_i$ (●) almost superimposed on those obtained during pulsing (■). Correspondingly, the mean value of the endogenous Ca^{2+} -binding capacity, κ_s , at high $[Ca^{2+}]_i$ is hardly distinguishable from that measured at low $[Ca^{2+}]_i$, during dye loading (Table 2). Subsequently, several trains of pulses were given at different times. The values of κ_s calculated during these trains support the notion that κ_s is not strongly dependent on $[Ca^{2+}]_i$ or on the length of time that the cell has been dialysed. These results imply that the endogenous buffer did not saturate when $[Ca^{2+}]_i$ was raised up to about 1 μM and, thus, that this buffer has a relatively low affinity for Ca^{2+} .

DISCUSSION

In this paper we have examined two interrelated aspects of Ca^{2+} signalling in single chromaffin cells: calcium gradients and calcium buffering. Digital imaging methods have directly demonstrated gradients in $[Ca^{2+}]_i$ during brief depolarizing pulses. These gradients are closely linked to the influx of Ca^{2+} through voltage-gated Ca^{2+} channels, because they rapidly dissipate when the channels are closed by repolarization or inactivation. Quantitative information from imaging has to be used with caution, however, since the indicator dye, which also is a mobile calcium buffer, may greatly influence the result (Sala & Hernandez-Cruz, 1990). Therefore Fura-2 was used as an exogenous Ca^{2+} buffer to estimate some of the properties of the endogenous cytoplasmic Ca^{2+} buffer of chromaffin cells. These estimates reveal that the endogenous buffer normally binds most of the Ca^{2+} that enters through the Ca^{2+} channels. However, because this buffer is immobile and has a relatively low affinity for Ca^{2+} , addition of a mobile, high-affinity buffer, such as Fura-2, allows the exogenous buffer to out-compete this endogenous buffer and greatly alter the nature of the depolarization-induced $[Ca^{2+}]_i$ signal.

Properties of the endogenous Ca^{2+} buffer

Two different methods based on competition between Fura-2 and the endogenous buffer for Ca^{2+} have been used to evaluate the properties of the endogenous Ca^{2+} buffer of chromaffin cells. Method 1, using measurements of the slowing of the time course of $[Ca^{2+}]_i$ removal following a stimulus, indicated that κ_s , the endogenous Ca^{2+} -binding capacity (bound calcium over free calcium), was 90. Method 2,

estimating the fraction of the incoming Ca^{2+} which is bound to Fura-2, yielded a κ_s value of 75. The latter value is definitely more accurate, since it rests on fewer assumptions, and has less scatter, experimentally. Although each method has limitations, the good correspondence between the two estimates supports the approach taken. The values indicate that 98–99% of all Ca^{2+} ions entering the chromaffin cells are rapidly bound to the endogenous cytoplasmic Ca^{2+} buffer. Studies of other neurone-line cells also indicate that cytoplasmic buffering exerts a substantial influence on the magnitude of the $[Ca^{2+}]_i$ signal (Gorman & Thomas, 1980; Smith & Zucker, 1980; McBurney & Neering, 1985; Ahmed & Connor, 1988; Thayer & Miller, 1990). Unfortunately, numerical values for binding capacity cannot easily be compared because previous estimates were either obtained in a different Ca^{2+} concentration range (Ahmed & Connor, 1988) or else the measurements were performed on a much slower time scale, such that slow buffering mechanisms contribute (Baker & Schlaepfer, 1978). However, our value is close to that (100) used by Smith & Zucker (1980) to fit fast Arsenazo III signals in *Aplysia* neurones (see also Gorman & Thomas, 1980). It is larger than the so-called 'expansion' E_i in frog skeletal muscle ($E_i = 16$; Melzer *et al.* 1986), but significantly smaller than the fast calcium-binding capacity observed in guinea-pig cardiac muscle (total calcium/free calcium > 1000; Wendt-Gallitelli & Isenberg, 1991).

The finding that the endogenous buffer is of low affinity explains another puzzling phenomenon seen both in our studies and in previous investigations on the time course of recovery of calcium signals (Ahmed & Connor, 1988; Thayer & Miller, 1990). The return to baseline following calcium influx is close to exponential over a surprisingly wide range of calcium concentrations. According to eqn (15), the time constant of relaxation should be a true constant only if κ_s is constant and if κ_B is negligible (since κ_B is highly dependent on $[Ca^{2+}]_i$ in the range of $[Ca^{2+}]_i$ variation). Thayer & Miller found exponential decays for $[Ca^{2+}]_i$ between 300 and 50 nM. If the endogenous buffer had an affinity of 150 nM (like Fura-2) or if Fura-2 had been the dominating buffer, the 'time constant' should have changed by a factor of 5 over this concentration range (eqns (12) and (15)). Constancy of the time constant is readily explained by constant κ_s , as found here, and by assuming that Fura-2 concentration was low enough not to significantly retard recovery.

Although cytoplasmic buffers are thought to play an important role in shaping $[Ca^{2+}]_i$ signals, very little is known about the specific identity of these buffers (Brinley, 1978; Baker & Schlaepfer, 1978). The measured properties of the endogenous Ca^{2+} buffer of chromaffin cells may provide some clues as to its chemical nature. One clue comes from its slow mobility, which indicates that it has an extremely large apparent molecular mass. The results shown in Table 1 indicate that the buffer capacity of a dialysed chromaffin cell does not change appreciably over more than 700 s of dialysis. A freely mobile, spherical molecule with a molecular mass of 1.6×10^6 Da would be expected to decrease to 1/e of its maximum concentration in this time, assuming a series conductance of 100 nS (Pusch & Neher, 1988). Thus, the fact that the endogenous Ca^{2+} buffer of chromaffin cells decreases much less dramatically over this time scale suggests an effective molecular mass in the order of 10^7 Da. This indicates that the buffer is either diffusible (and has a mass in the order of an organelle) or that it is anchored to prevent movement (and could have a smaller mass). Some of the annexins are likely candidates in this respect.

Unlike in the case of neutrophils (von Tscharner, Deranleau & Baggiolini, 1986) the endogenous Ca^{2+} buffer in chromaffin cells does not show any signs of saturation for $[\text{Ca}^{2+}]_i$ up to $1 \mu\text{M}$ (Table 2). This suggests that the buffer has a low affinity for Ca^{2+} ions. Our value of κ_s is compatible with $375 \mu\text{M}$ of buffer at $5 \mu\text{M}$ affinity, or $750 \mu\text{M}$ at $10 \mu\text{M}$ affinity. This excludes Ca^{2+} -binding proteins such as parvalbumins, which have Ca^{2+} affinities in the submicromolar range (Ebashi & Ogawa, 1988), and is marginally compatible with calmodulins. More likely would be molecules such as annexins, which are present in chromaffin cells and have Ca^{2+} affinities as low as

TABLE 2. Endogenous calcium binding capacities at different $[\text{Ca}^{2+}]_i$ values and times
Pulse train

	Loading	1	2	3	4
Time (s)	150	350	790	1080	1660
Mean $[\text{Ca}^{2+}]_i$ (μM)	0.18	0.71	0.64	1.13	0.95
Mean κ_s	70	67 ± 8	51 ± 6	96 ± 13	89 ± 12

All values are from one cell. Time is the mean time after patch rupture for the pulses of a given train. Mean calcium is the mean of mean values in $[\text{Ca}^{2+}]_i$ during steps. Errors, where given, are s.e.m.'s.

hundreds of micromolar (Pollard, Burns & Rojas, 1988; Creutz, Drust, Martin, Kambouris, Snyder & Hamman, 1988). Also the troponin-C-like Ca^{2+} -binding protein isolated from adrenal medulla (Kuo & Coffee, 1976) has an affinity compatible with our findings, but, according to its abundance, it represents only a minor fraction of the total calcium binding capacity.

Implications for measurement of $[\text{Ca}^{2+}]_i$ signals

The observation that Fura-2 can compete effectively with endogenous Ca^{2+} buffers sets some limits on the use of this dye as a cytoplasmic Ca^{2+} indicator. If the goal is to measure changes in free calcium concentration undisturbed by the presence of the indicator dye, then the method of choice is the ratio method as described by Grynkiewicz *et al.* (1985) and the calcium binding capacity of Fura-2 should be smaller than that of the endogenous buffer. If, however, the goal is to measure Ca^{2+} fluxes into the cytoplasmic compartment at fixed $[\text{Ca}^{2+}]_i$, then the intracellular concentration of Fura-2 should be high to ensure that all of the Ca^{2+} load is taken up by the Fura-2. Under such conditions, the magnitude of the Ca^{2+} flux is proportional to the absolute fluorescence changes at the Ca^{2+} -sensitive wavelength (eqn (39)). The two measurements are complementary in the same way as are current clamp and voltage clamp measurements. What should be avoided is an intermediate situation, where fluorescence signals will give only qualitative hints. In the case of chromaffin cells, $400 \mu\text{M}$ -Fura-2 seems to be adequate for measurement of Ca^{2+} fluxes elicited by brief depolarizations (Fig. 8A). In the case of $[\text{Ca}^{2+}]_i$ measurements, the magnitude of the signal is inversely related to the sum of κ_B and κ_s (eqn (21)), so that κ_B should be no more than 10% of κ_s if the $[\text{Ca}^{2+}]_i$ signal is to be within 90% of its normal value. For chromaffin cells, with a κ_s of about 75, then κ_B should be no more than 7.5, which would require a Fura-2 concentration of no more than $75 \mu\text{M}$ for a $[\text{Ca}^{2+}]_i$ signal of $1 \mu\text{M}$ (eqn (12)). For smaller Ca^{2+} signals the requirement is more stringent.

For instance, for Ca^{2+} signals comparable in magnitude to the K_D of Fura-2 (which was found to be $0.15 \mu\text{M}$ in chromaffin cell cytoplasm), the limiting Fura-2 concentration would be approximately $4 \mu\text{M}$, and $38 \mu\text{M}$ -Fura-2 would double the endogenous calcium-binding capacity. This result is very similar to that of Timmerman & Ashley (1986) who found that $30 \mu\text{M}$ -Fura-2 almost doubles the relaxation time of force in striated muscle.

Spatially resolved measurements require even more stringent criteria. For a faithful report on the spatiotemporal pattern of Ca^{2+} changes, the indicator should not only not bind significant amounts of calcium, but also not contribute to its redistribution. In the absence of mobile endogenous buffers, the only diffusing calcium atoms are those free and those bound to Fura-2. The flux of calcium j_{Ca} through any small volume element of length Δx can then be written as:

$$j_{\text{Ca}} = -D_{\text{Ca}} \frac{\Delta[\text{Ca}^{2+}]_i}{\Delta x} - D_{\text{BCa}} \frac{\Delta[\text{BCa}]}{\Delta x}, \quad (40)$$

where D_{Ca} and D_{BCa} are diffusion coefficients of calcium and BCa (the calcium loaded form of exogenous buffer), respectively. Free calcium is known to diffuse slowly in cytoplasm (Hodgkin & Keynes, 1957), such that D_{Ca} and D_{BCa} can be considered roughly equal. Then, the contributions of the two terms in eqn (40) to total calcium flux are proportional to the local gradients of the respective chemical species. Assuming $[\text{Ca}^{2+}]_i$ values of $1 \mu\text{M}$ near the membrane and $0.1 \mu\text{M}$ in the centre, and a total Fura-2 concentration of $10 \mu\text{M}$, one would expect approximately $9 \mu\text{M}$ of Ca^{2+} -bound Fura-2 near the membrane and $4\text{--}5 \mu\text{M}$ in the centre of the cell (after Fura-2- Ca^{2+} equilibration, which is rapid). Thus, even this minute amount of Fura-2 would dominate the redistribution process. This effect of a mobile chelator also has been demonstrated in the model calculations of Sala & Hernandez-Cruz (1990).

The above discussion assumes a complete absence of mobile endogenous buffers, as suggested by our measurements. The measurements cannot totally exclude, however, the presence of some amounts of mobile buffers, since the present protocol only allows reliable measurements of κ_s after some Fura-2 has diffused into the cell. A small amount of highly mobile buffer which would escape in that time span might have been overlooked.

The considerations discussed in the previous paragraphs suggest that an extremely low concentration of Fura-2 is needed to accurately depict the spatial profile of the $[\text{Ca}^{2+}]_i$ changes occurring during depolarization. However, our imaging experiments required substantially higher concentrations of Fura-2 ($100\text{--}500 \mu\text{M}$) in order to have sufficient fluorescence for measurement with the video camera. At these concentrations, it is likely that the Fura-2 is distorting the spatial gradients and is causing them to collapse more rapidly than in an unperturbed cell. The limited temporal and spatial resolution of the imaging method (Fig. 1) would lead to a further underestimation of the steepness of these gradients. For example, although depolarization is thought to raise $[\text{Ca}^{2+}]_i$ levels at the release sites to $10\text{--}100 \mu\text{M}$ (Augustine & Neher, 1992), the highest levels measurable with the imaging method are in the order of $1 \mu\text{M}$ (e.g. Fig. 4). This presumably is due to the fact that the $[\text{Ca}^{2+}]_i$ gradients at the release sites drop off over dimensions of a fraction of a

micrometre (Chad & Eckert, 1984; Simon & Llinas, 1985; Fogelson & Zucker, 1985; Sala & Hernandez-Cruz, 1990), while the spatial resolution of our system is of the order of a few micrometres (Fig. 1A). In addition, these highly localized gradients should dissipate much more rapidly than the 100 ms time resolution of our system, some of this fast dissipation being due to the mobility of Fura-2. In the centre of the cell, however, where the separation from the Ca^{2+} sources would cause the $[\text{Ca}^{2+}]_i$ gradients to change more gradually as a function of time and space (e.g. Sala & Hernandez-Cruz, 1990), imaging measurements might provide more reliable estimates of the magnitude of $[\text{Ca}^{2+}]_i$ changes, if the Fura-2 concentration can be kept sufficiently low.

In conclusion, radial gradients in $[\text{Ca}^{2+}]_i$ occur during depolarization, due to the localization of the voltage-gated Ca^{2+} channels in the plasma membrane, but the steepness of these gradients is underestimated during imaging measurements. In the small volume just beneath the plasma membrane, $[\text{Ca}^{2+}]_i$ appears to reach levels in the order of 10–100 μM (Augustine & Neher, 1992), while in the central region of the cell, $[\text{Ca}^{2+}]_i$ approaches levels in the order of 1 μM (e.g. Figs 5 and 6). Because of the large volume of the interior of the cell compared to the submembranous region, photomultipliers, fluorimeters, flow cytometers and other devices that measure average $[\text{Ca}^{2+}]_i$ will measure changes of relatively small magnitude that correspond to those occurring in the central region. Accurate definition of the true dimensions of these intracellular gradients will require methods with resolution and sensitivity substantially better than the video microscope that we have used.

Release of calcium from intracellular stores?

Several investigators have observed release of calcium from intracellular stores (Lipscombe *et al.* 1988; O'Sullivan *et al.* 1989; Hernandez-Cruz *et al.* 1990) as part of the depolarization-induced calcium signal. The close quantitative agreement between calcium influx, as measured by current, and that detected by Fura-2 fluorescence reported here leaves little room for such release in our study (see also Thayer & Miller, 1990). Further, our imaging experiments suggest that the depolarization induced elevation of $[\text{Ca}^{2+}]_i$ originated in the vicinity of the plasma membrane (Fig. 4), while calcium released from intracellular stores often appears first in the interior of the cell (e.g. O'Sullivan *et al.* 1989). It might be argued that we had to buffer calcium quite strongly in all the experiments aimed at quantitative flux measurements and, thus, prevented 'calcium-induced calcium release'. However, the agreement between theory and experiments also extends to responses during the loading and unloading episodes (Figs 8 and 10) where exogenous buffer had much less buffering power. If there had been any significant contributions from intracellular release, it should have shown up in the form of marked deviations from the binding curves displayed in Fig. 10, or as humps in the time courses of recovery. Such humps were, indeed, seen occasionally following excessive stimulation with long-pulse trains (not shown); but single pulses up to 2 s in duration never produced such a response. Release of intracellular calcium may, thus, occur with intense long-term stimulation, such as with K^+ -depolarization, but it is probably not associated with single action potentials in bovine chromaffin cells.

We thank R. S. Zucker for valuable comments on the manuscript and M. Papke and M. Pilot for preparing the chromaffin cells. This work was supported in part by NIH grant NS-21624 and a fellowship from the Humboldt Foundation to G.A. and by a grant from the Deutsche Forschungsgemeinschaft to E.N.

REFERENCES

- AHMED, Z. & CONNOR, J. A. (1988). Calcium regulation by and buffer capacity of molluscan neurons during calcium transients. *Cell Calcium* **9**, 57–69.
- ARMSTRONG, C. M. & BEZANILLA, F. (1977). Inactivation of the sodium channel. II. Gating current experiments. *Journal of General Physiology* **70**, 567–590.
- AUGUSTINE, G. J., CHARLTON, M. P. & SMITH, S. J. (1987). Calcium action in synaptic transmitter release. *Annual Review of Neuroscience* **10**, 633–693.
- AUGUSTINE, G. J. & NEHER, E. (1990). Imaging calcium transients in patch clamped chromaffin cells. *Society of Neuroscience Abstracts* **16**, 1013.
- AUGUSTINE, G. J. & NEHER, E. (1992). Calcium requirements for secretion in bovine chromaffin cells. *Journal of Physiology* **450**, 247–271.
- BAKER, P. F. & SCHLAEPFER, W. W. (1978). Uptake and binding of calcium by axoplasm isolated from giant axons of *Loligo* and *Myxicola*. *Journal of Physiology* **276**, 103–125.
- BRINLEY, F. J. JR (1978). Calcium buffering in squid axons. *Annual Review of Biophysics and Bioengineering* **7**, 363–392.
- BURGOYNE, R. D., CHEEK, T. R., MORGAN, A., O'SULLIVAN, A. J., MORETON, R. B., BERRIDGE, M. J., MATA, A. M., COLYER, J., LEE, A. G. & EAST, J. M. (1989). Distribution of two distinct Ca^{2+} -ATPase-like proteins and their relationships to the agonist sensitive calcium store in adrenal chromaffin cells. *Nature* **342**, 72–74.
- CHAD, J. E. & ECKERT, R. O. (1984). Calcium domains associated with individual channels can account for anomalous voltage relations of Ca-dependent responses. *Biophysical Journal* **45**, 993–999.
- CLAPHAM, D. E. & NEHER, E. (1984). Trifluoperazine reduces inward ionic currents and secretion by separate mechanisms in bovine chromaffin cells. *Journal of Physiology* **353**, 541–564.
- CREUTZ, C. E., DRUST, D. S., MARTIN, W. H., KAMBOURIS, N. G., SNYDER, S. L. & HAMMAN, H. C. (1988). Calcium-dependent membrane-binding proteins as effectors of secretion in mammalian and fungal cells. In *Molecular Mechanisms in Secretion*, Alfred Benzon Symposium 25, ed. THORN, N. A., TREIMAN, M. & PETERSON, O. H., pp. 575–590. Munksgaard, Copenhagen.
- DOUGLAS, W. W. (1968). Stimulus-secretion coupling: the concept and clues from chromaffin and other cells. *British Journal of Pharmacology* **34**, 451–474.
- EBASHI, S. & OGAWA, Y. (1988). Troponin C and calmodulin as calcium receptors. Mode of action and sensitivity to drugs. In *Calcium in Drug Actions*, ed. BAKER, P. F., pp. 32–56. Springer, Berlin.
- FENWICK, E. M., MARTY, A. & NEHER, E. (1982). Sodium and calcium channels in bovine chromaffin cells. *Journal of Physiology* **331**, 599–635.
- FOGELSON, A. L. & ZUCKER, R. S. (1985). Presynaptic calcium diffusion from various arrays of single channels. *Biophysical Journal* **48**, 1003–1017.
- GORMAN, A. L. F. & THOMAS, M. V. (1980). Intracellular calcium accumulation during depolarization in a molluscan neurone. *Journal of Physiology* **308**, 259–285.
- GRYNKIEWICZ, G., POENIE, M. & TSIEN, R. Y. (1985). A new generation of Ca^{2+} indicators with greatly improved fluorescence properties. *Journal of Biological Chemistry* **260**, 3440–3450.
- HERNANDEZ-CRUZ, A., SALA, F. & ADAMS, P. R. (1990). Subcellular calcium transients visualized by confocal microscopy in a voltage-clamped vertebrate neuron. *Science* **247**, 858–862.
- HIRAOKA, Y., SEDAT, J. W. & AGARD, D. A. (1990). Determination of three-dimensional imaging properties of a light microscope system. Partial confocal behaviour in epifluorescence microscopy. *Biophysical Journal* **57**, 325–333.
- HODGKIN, A. & KEYNES, R. D. (1957). Movement of labelled calcium in squid giant axons. *Journal of Physiology* **138**, 253–281.
- HOSHI, T., ROTHLEIN, J. & SMITH, S. J. (1984). Facilitation of Ca^{2+} -channel currents in bovine adrenal chromaffin cells. *Proceedings of the National Academy of Sciences of the USA* **81**, 5871–5875.

- INOUE, S. (1986). *Video Microscopy*. Plenum Press, New York.
- KAO, J. P. Y. & TSIEN, R. Y. (1988). Ca^{2+} binding kinetics of fura-2 and azo-1 from temperature-jump relaxation measurements. *Biophysical Journal* **53**, 635-639.
- KASAI, H. & AUGUSTINE, G. J. (1990). Cytosolic Ca^{2+} gradients triggering unidirectional fluid secretion from exocrine pancreas. *Nature* **348**, 735-738.
- KATZ, B. (1969). *The Release of Neural Transmitter Substances*. Liverpool University Press, Liverpool.
- KIM, Y. I. & NEHER, E. (1988). IgG from patients with Lambert-Eaton syndrome blocks voltage-dependent calcium channels. *Science* **239**, 405-408.
- KNIGHT, D. E. & KESTVEN, N. T. (1983). Evoked transient intracellular free Ca^{2+} changes and secretion in isolated bovine adrenal medullary cells. *Proceedings of the Royal Society B* **218**, 177-199.
- KUO, I. C. & COFFEE, C. J. (1976). Purification and characterization of a troponin-C-like protein from bovine adrenal medulla. *Journal of Biological Chemistry* **251**, 1603-1609.
- LIPSCOMBE, D., MADISON, D. V., POENIE, M., REUTER, H., TSIEN, R. W. & TSIEN, R. Y. (1988). Imaging of cytosolic Ca^{2+} transients arising from Ca^{2+} stores and Ca^{2+} channels in sympathetic neurons. *Neuron* **1**, 355-365.
- MATHIAS, R. T., COHEN, I. S. & OLIVA, C. (1990). Limitations of the whole cell patch clamp technique in the control of intracellular concentrations. *Biophysical Journal* **58**, 759-770.
- McBURNIE, R. N. & NEERING, V. (1985). The measurement of changes in intracellular free calcium during action potentials in mammalian neurones. *Journal of Neuroscience Methods* **13**, 65-76.
- MELZER, W., RIOS, E. & SCHNEIDER, M. F. (1986). The removal of myoplasmic free calcium following calcium release in frog skeletal muscle. *Journal of Physiology* **372**, 261-292.
- NEHER, E. (1989). Combined Fura-2 and patch-clamp measurements in rat peritoneal mast cells. In *Neuromuscular Junction* **5**, ed. SELLIN, L. C., LIBELIUS, R. & THESLEFF, S., pp. 65-76. Elsevier, Amsterdam.
- O'SULLIVAN, A. J., CHEEK, T. R., MORETON, R. B., BERRIDGE, M. J. & BURGOYNE, R. D. (1989). Localization and heterogeneity of agonist-induced changes in cytosolic calcium concentration in single bovine adrenal chromaffin cells from video imaging of Fura-2. *EMBO Journal* **8**, 401-411.
- PARNAS, H., DUDEL, J. & PARNAS, I. (1982). Neurotransmitter release and its facilitation in crayfish. I. Saturation kinetics of release and of entry and removal of calcium. *Pflügers Archiv* **393**, 1-14.
- PENNER, R. & NEHER, E. (1988). The role of calcium in stimulus-secretion coupling in excitable and non-excitable cells. *Journal of Experimental Biology* **139**, 329-345.
- POCOCK, G. (1983). Ion movement in isolated bovine adrenal medullary cells treated with ouabain. *Molecular Pharmacology* **23**, 681-697.
- POLLARD, H. B., BURNS, A. L. & ROJAS, E. (1988). A molecular basis for synexin-driven, calcium-dependent membrane fusion. *Journal of Experimental Biology* **139**, 267-286.
- PUSCH, M. & NEHER, E. (1988). Rates of diffusional exchanges between small cells and a measuring patch pipette. *Pflügers Archiv* **411**, 204-211.
- SALA, F. & HERNANDEZ-CRUZ, A. (1990). Calcium diffusion modeling in a spherical neuron. Relevance of buffering properties. *Biophysical Journal* **57**, 313-324.
- SIMON, S. M. & LLINAS, R. R. (1985). Compartmentalization of the submembrane calcium activity during calcium influx and its significance in transmitter release. *Biophysical Journal* **48**, 485-498.
- SMITH, S. J. & ZUCKER, R. S. (1980). Aequorin response facilitation and intracellular calcium accumulation in molluscan neurones. *Journal of Physiology* **300**, 167-196.
- SMITH, S. J., OSSES, L. R. & AUGUSTINE, G. J. (1988). Fura-2 imaging of localized calcium accumulation within squid 'giant' presynaptic terminals. In *Calcium and Ion Channel Modulation*, ed. GRINNELL, A. D., ARMSTRONG, D. & JACKSON, M. B., pp. 147-155. Plenum Press, New York.
- THAYER, S. A. & MILLER, R. J. (1990). Regulation of the intracellular free calcium concentration in single rat dorsal root ganglion neurones *in vitro*. *Journal of Physiology* **425**, 85-115.
- TILLOTSON, D. & NASI, E. (1988). Ca^{2+} diffusion in the cytoplasm of *Aplysia* neurons: its relationship to local concentration changes. In *Calcium and Ion Channel Modulation*, ed. GRINNELL, A. D., pp. 133-146. Plenum Press, New York.
- TIMMERMAN, M. P. & ASHLEY, C. C. (1986). Fura-2 diffusion and its use as an indicator of transient free calcium changes in single striated muscle cells. *FEBS Letters* **209**, 1-8.
- TSIEN, R. Y. & POENIE, M. (1986). Fluorescence ratio imaging: a new window into intracellular ionic signalling. *Trends in Biological Sciences* **11**, 450-455.
- VON TSCHARNER, V., DERANLEAU, D. A. & BAGGIOLINI, M. (1986). Calcium fluxes and calcium buffering in human neutrophils. *Journal of Biological Chemistry* **261**, 10163-10168.
- WENDT-GALLITELLI, M. F. & ISENBERG, G. (1991). Total and free myoplasmic calcium during a contraction cycle: X-ray microanalysis in guinea-pig ventricular myocytes. *Journal of Physiology* **435**, 349-372.
- WILLIAMS, D. A., FOGARTY, K. E., TSIEN, R. Y. & FAY, F. S. (1985). Calcium gradients in single smooth muscle cells revealed by the digital imaging microscope using Fura-2. *Nature* **313**, 558-561.
- ZUCKER, R. S. (1989). Models of calcium regulation in neurons. In *Neuronal Models of Plasticity*, ed. BYRNE, J. H. & BERRY, W. O., pp. 403-422. Academic Press, Orlando, FL, USA.